

Multilingual Training-Free Remote Sensing Image Captioning

Carlos Rebelo[✉], Gil Rocha[✉], João Daniel Silva[✉], Bruno Martins[✉]

Abstract—Remote sensing image captioning has advanced rapidly through encoder–decoder models, although the reliance on large annotated datasets and the focus on English restricts global applicability. To address these limitations, we propose the first training-free multilingual approach, based on retrieval-augmented prompting. For a given aerial image, we employ a domain-adapted SigLIP2 encoder to retrieve related captions and few-shot examples from a datastore, which are then provided to a language model. We explore two variants: an image-blind setup, where a multilingual Large Language Model (LLM) generates the caption from textual prompts alone, and an image-aware setup, where a Vision–Language Model (VLM) jointly processes the prompt and the input image. To improve the coherence of the retrieved content, we introduce a graph-based re-ranking strategy using PageRank on a graph of images and captions. Experiments on four benchmark datasets across ten languages demonstrate that our approach is competitive with fully supervised English-only systems and generalizes to other languages. Results also highlight the importance of re-ranking with PageRank, yielding up to 35% improvements in performance metrics. Additionally, it was observed that while VLMs tend to generate visually grounded but lexically diverse captions, LLMs can achieve stronger BLEU and CIDEr scores. Lastly, directly generating captions in the target language consistently outperforms other translation-based strategies. Overall, our work delivers one of the first systematic evaluations of multilingual, training-free captioning for remote sensing imagery, advancing toward more inclusive and scalable multimodal Earth observation systems.

Index Terms—Remote Sensing, Few-shot Learning, Retrieval Augmented Generation, Multilingual Captioning

I. INTRODUCTION

REMOTE sensing image captioning, i.e. the task of generating textual descriptions for aerial images, has seen significant progress through encoder-decoder models. However, the reliance on large annotated training datasets, and the prevailing focus on the English language, limits the accessibility and applicability of this technology for a global user base.

Instead of adhering to the conventional supervised training paradigm, we propose a training-free approach for multilingual captioning that does not require manually annotated data for model training. Our method instead hinges on prompting a multilingual Large Language Model (LLM) with captions from similar images to the input image. This aligns with recent findings demonstrating that retrieval-based prompting can achieve state-of-the-art performance with LLMs, bypassing the need for large-scale multimodal training data [1]–[3].

Our primary contribution is the application and analysis of a few-shot methodology within the remote sensing domain and

in a multilingual setting. Specifically, for a given aerial image, we employ a SigLIP2 encoder [4], fine-tuned for the remote sensing domain, to retrieve relevant captions and similar images, which also have relevant captions associated, forming few-shot examples. All these captions are then consolidated into a prompt to guide the language model in generating the final description. We explore two variants of this approach, namely an image-blind version that provides only the textual prompt to a Large Language Model (LLM), and an image-aware version that supplies both the prompt and the input image to a Vision-Language Model (VLM).

To enhance the quality and coherence of the information used in the prompt, we also introduce a novel graph-based re-ranking strategy. This method leverages the personalized PageRank algorithm [5], [6] on a multimodal graph where retrieved images and captions are represented as nodes. Node and edge weights are determined by their similarity to the target image and to each other, computed using the same visual encoder from the retrieval stage. This process re-ranks the retrieved elements to better capture their collective relevance, which we hypothesize to lead to more effective prompts.

Experiments on established benchmark datasets demonstrate that our approach is competitive with fully supervised English-only models, all while enabling multilingual captioning without any dedicated training. Furthermore, our analysis confirms that the graph-based re-ranking strategy yields significant improvements, by enhancing the semantic coherence of the elements within the prompt.

In summary, we propose a multilingual remote sensing image captioning method that leverages cross-modal retrieval to prompt large-scale language and vision-language models. The main contributions of this work are as follows:

- We demonstrate that our approaches, both image-blind (using LLMs) and image-aware (using VLMs), achieve results that are competitive with fully-supervised methods for English remote sensing image captioning.
- We provide one of the first systematic evaluations of remote sensing image captioning in a multilingual setting, showing consistent performance across languages.
- We propose a graph-based re-ranking strategy to improve the coherence of retrieved information for prompting, and we experimentally validate its effectiveness.

The rest of this paper is organized as follows: Section II surveys related work, while Section III describes the proposed approach. Section IV details the experimental setup, including the considered datasets and evaluation metrics, and Section V reports the obtained results. Finally, Section VI summarizes the main conclusions and discusses directions for future work.

The authors are with INESC-ID, Lisboa, Portugal. Carlos Rebelo (e-mail: carlosrebelo17@tecnico.ulisboa.pt), João Daniel Silva and Bruno Martins are also with Instituto Superior Técnico, Universidade de Lisboa, Portugal. Gil Rocha is also with Faculdade de Engenharia da Universidade do Porto, Portugal.

II. RELATED WORK

The interaction between natural language and images is nowadays a popular topic within the machine learning, natural language processing, and computer vision communities, where researchers have worked on problems such as cross-modal retrieval, visual question answering, referring expression segmentation, or image captioning. Addressing these problems is particularly relevant in the context of remote sensing [7], given that the current volume of remotely sensed Earth Observation (EO) data clearly motivates the development of vision-and-language methods that can support natural language interactions with large EO image repositories.

Models based on Contrastive Language-Image Pre-training (CLIP) and Sigmoid Language-Image Pre-training (SigLIP) are nowadays extensively used in a variety of vision-and-language tasks [4], [8], e.g. as dual encoders that can support cross-modal retrieval, or as vision encoders within larger models. In brief, CLIP models are based on an architecture with two separate encoders, one for visual inputs and one for textual inputs, trained on large-scale datasets with a contrastive objective that encourages semantically similar concepts, across both modalities, to be aligned in the shared representation space. The main difference between CLIP and SigLIP lies in the training objective: while CLIP employs a contrastive loss, SigLIP uses a sigmoid-based loss that treats each image-text pair independently. Despite this distinction, both approaches share the same overall architecture and the aim of learning a joint embedding space. Motivated by the strong results in tasks involving generalist images, the adaptation of CLIP to specific domains is currently being actively researched. In the specific domain of remote sensing, recent efforts include RemoteCLIP [9] or RS-M-CLIP [10], achieving very strong results in tasks such as cross-modal retrieval or zero-shot image classification.

CLIP vision encoders are also commonly used as backbones within recent architectures leveraging LLMs for vision-and-language tasks. For instance, LLaVA [11], MiniGPT-v2 [12], or InstructBLIP [13] are examples of instruction fine-tuned models supporting conversation and reasoning over visual inputs, connecting a CLIP vision encoder to a pre-trained LLM, and using supervised learning to train the cross-modal connections. Considering the remote sensing domain, similar efforts include RSGPT [14], GeoChat [15], SkyEyeGPT [16], LHRs-Bot [17], or TEOChat [18]. Models like these address not only image captioning, which is the focus of the present study, but also other multimodal tasks (e.g., visual question answering) through a common interface based on prompting the models with task-specific instructions. However, specialized encoder-decoder models for image captioning correspond to the current state-of-the-art [19], in some cases combining image encoders based on CLIP together with modules specifically designed to handle the properties of remote sensing imagery. For instance, models like MLCA-Net [20], HCNet [21], MC-Net [22], BITA [23], the Aware-Transformer [24], or the Deformable Transformer [25] all contain specialized modules to adaptively aggregate image features of multiple scales and specific regions.

Despite the strong empirical results, all the aforementioned models depend on large datasets pairing aerial images to captions for supervised training. Extending these methods to multilingual settings is particularly challenging, requiring annotated data covering each target language, and larger models to mitigate the curse of multilinguality. Some previous studies have alternatively proposed training-free strategies for connecting vision encoders to LLMs. For instance, Socratic models [26] correspond to a generalist framework in which an LLM is used to process a prompt that integrates information from different models. Under this framework, a task like image captioning can be performed using a CLIP model to retrieve different concepts from an input image (e.g., locations or objects that are likely featured in the image), and then prompting an LLM with the retrieved information. More recently, building on earlier approaches for retrieval-augmented generation of image captions [27], [28], Language Model Prompt-based Captioning (LMCap) considered a similar strategy [2], addressing multilingual image captioning through the use of CLIP to retrieve similar captions from a datastore of examples, which are then used to prompt an LLM into generating the target caption. Experimental results showed that LMCap largely outperformed a Socratic modeling approach and performed competitively against supervised approaches for multilingual image captioning, without requiring expensive training with large-scale multimodal data.

This paper essentially describes the application of LMCap to the domain of remote sensing imagery, using a SigLIP2 visual encoder and at the same time extending this approach in several directions. The extensions include a graph-based re-ranking strategy with personalized PageRank [5], [6], and a new image-aware approach, that uses VLMs instead of LLMs, and with the input image being prompted together with the retrieved information. The following section details the general procedure and also the proposed extensions.

III. PROPOSED APPROACH

This section introduces our multilingual training-free captioning framework for remote sensing imagery, designed around retrieval-augmented generation. The framework can be used in two complementary modes: an image-blind strategy, where captions are produced without directly encoding the input image, and an image-aware strategy, where the input image is also provided to a frozen vision-language model. Both modes rely on a common retrieval and re-ranking backbone, diverging only at the final stage, when prompting the generative model.

The process starts by retrieving semantically related captions from a large corpus using a domain-adapted SigLIP2 encoder (Section III-A). The same encoder is then employed to retrieve visually similar images, whose captions serve as few-shot demonstrations of the captioning task (Section III-B). For each of the similar images, additional captions are collected along with their gold-standard annotations, in order to build the demonstrations. To enhance both coherence and diversity, the retrieved material is reorganized through a graph-based re-ranking procedure that applies personalized PageRank to

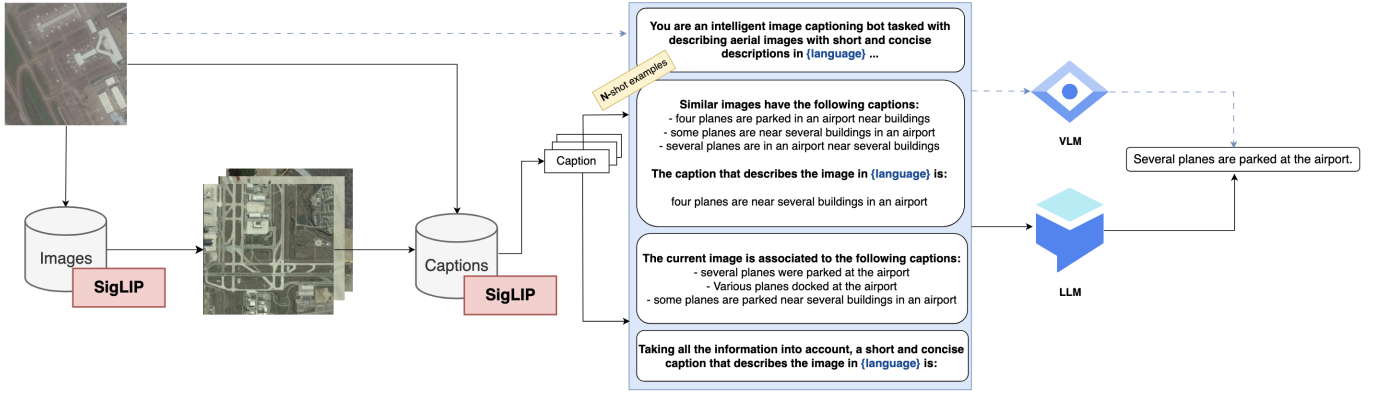


Fig. 1: A general illustration for the proposed image captioning approach. For a given input image, the system first retrieves related captions, plus the most similar images and, for each of the images, also the corresponding most similar captions. The retrieved information is then assembled into a prompt, which can either be provided alone to a multilingual LLM (solid line) or, together with the input image, to a multilingual VLM (dashed line). In both cases, the model generates a caption in the target language. The prompt illustrated in the figure is a simplified example.

emphasize semantically central items (Section III-C). Finally, the re-ranked examples and captions are arranged into a prompt (Section III-D). In the image-blind mode, this prompt is given to a multilingual LLM, which generates the caption without visual access. In the image-aware mode, the prompt is processed by a VLM that jointly considers the image and the retrieved textual context. An overview of both modes for the proposed pipeline is shown in Figure 1.

A. Retrieving Similar Captions

The proposed approach begins by retrieving captions that are semantically related to the input image, which are later used to construct a prompt for the language model. This retrieval step is based on version of the SigLIP2 [4] model that was fine-tuned for the remote sensing domain, here called RS-SigLIP2. This model was fine-tuned in previous work using the same procedure as RS-M-CLIP [10]. Similarly to other CLIP-style models, RS-SigLIP2 incorporates aligned image and text encoders, denoted by f_ϕ and g_ϕ , which map inputs into a shared multimodal embedding space.

First, a datastore $\mathcal{D} = \{\hat{\mathbf{x}}_i, \hat{\mathbf{y}}_i\}_{i=1}^M$ is built from a large set of remote sensing images, paired to captions in the English language, with M image-caption pairs. The datastore indexes vector representations produced by RS-SigLIP2 for each image $f_\phi(\hat{\mathbf{x}}_i) = \hat{\mathbf{v}}_i \in \mathbb{R}^d$ and each caption $g_\phi(\hat{\mathbf{y}}_i) = \hat{\mathbf{u}}_i \in \mathbb{R}^d$.

At inference time, the input image is also encoded with the RS-SigLIP2 model (i.e., $f_\phi(\mathbf{x}_z) = \mathbf{v}_z$), and the image representation is used to retrieve the most similar captions. The similarity is obtained by calculating the cosine similarity between the vector representation of the image and each caption i on the datastore \mathcal{D} , expressed by $\text{sim}(\mathbf{x}_z, \hat{\mathbf{y}}_i) = \cos(f_\phi(\mathbf{x}_z), g_\phi(\hat{\mathbf{y}}_i))$. These captions will serve to guide a language model as examples of what the caption to be generated should resemble, through the use of the prompt detailed in Section III-D. Based on the computed similarities, we retrieve the top-10 captions from the datastore. While the final prompt used to query the language model will only contain the top- $k \leq 10$ captions, as

determined through experiments, we initially retrieve the top-10 most similar captions considering this pool for the graph-based re-ranking algorithm based on PageRank.

B. Retrieving Few-Shot Examples

To obtain few-shot examples, we rely on the image encoder f_ϕ from RS-SigLIP2 to embed the input image \mathbf{x}_z , producing the feature vector $f_\phi(\mathbf{x}_z) = \mathbf{v}_z$. Cosine similarities are then computed between \mathbf{v}_z and all image embeddings stored in the datastore \mathcal{D} , denoted $\hat{\mathbf{v}}_p$, from which the ten most similar images $\hat{\mathbf{x}}_p$ are retrieved. The captions associated to these images are retained to build candidate few-shot demonstrations for the prompt. Ten candidates are selected rather than directly retrieving the final N few-shot examples, so that they can later be reranked through the PageRank procedure described in Section III-C.

For each of the retrieved images, we also retrieve the most similar captions from \mathcal{D} , using the same cross-modal similarity computation described in Section III-A, i.e., based on $\text{sim}(\hat{\mathbf{x}}_p, \hat{\mathbf{y}}_i) = \cos(f_\phi(\hat{\mathbf{x}}_p), g_\phi(\hat{\mathbf{y}}_i))$. The set of ground-truth captions $\hat{\mathbf{y}}_k$ associated with each similar image $\hat{\mathbf{x}}_p$ is also ranked according to similarity towards $\hat{\mathbf{x}}_p$. We filter the results so that the ground-truth captions, associated to the examples, differ from the retrieved captions referred to in the previous paragraph. The example images, together with the ranked and filtered similar captions and ground-truth captions, are included in the pool of candidate few-shot examples, and treated as nodes in a semantic-visual graph, which is later processed to refine the prompt composition.

Note that the goal of the few-shot examples is to illustrate how the captioning task should be performed. Consequently, in a multilingual setting, the selected ground-truth captions should be presented in the target language. Since all captions in the datastore \mathcal{D} are originally in English, we employ a machine translation model to convert the selected captions into the target language. Further details regarding the translation approach are provided in Section IV-C.

C. Re-ranking with PageRank

A key novelty of our method is a graph-based re-ranking mechanism designed to enhance the coherence of the retrieved content supplied to the language model. Since our approach relies on retrieved captions and few-shot examples, the quality of this context is paramount. A naive selection of these items can introduce redundancy or inconsistencies. To address this, we adapt the personalized PageRank algorithm [5], [6]. This allows us to re-rank the retrieved content by considering not only each item’s individual relevance to the query image, but also the semantic interrelations within the entire set. We construct a fully connected graph where each retrieved element (e.g., a candidate caption or a few-shot example component) is a node. The input query image, while not a node itself, guides the ranking process through a personalization vector.

The graph’s structure is formally defined by a row-stochastic adjacency matrix $W \in \mathbb{R}^{n \times n}$. The weight W_{ij} between two nodes is derived from the cosine similarity of their multimodal embeddings, \mathbf{e}_i and \mathbf{e}_j , as produced by RS-SigLIP2:

$$W_{ij} = \frac{\max(\cos(\mathbf{e}_i, \mathbf{e}_j), 0)}{\sum_{k=1}^n \max(\cos(\mathbf{e}_i, \mathbf{e}_k), 0)}. \quad (1)$$

This ensures that the edge weights are normalized for the stochastic random walk model. The “personalization” is achieved through a vector \mathbf{v} , which biases the ranking towards nodes most relevant to the input image. Each component v_i is proportional to the similarity s_i between the content of node i and the input image:

$$v_i = \frac{\max(s_i, 0)}{\sum_{j=1}^n \max(s_j, 0)}. \quad (2)$$

The final scores are captured in the PageRank vector \mathbf{r} , calculated as the fixed point of the following iterative update:

$$\mathbf{r} = \alpha W^T \mathbf{r} + (1 - \alpha) \mathbf{v}, \quad (3)$$

where $\alpha \in (0, 1)$ is a damping factor that balances the influence of the graph’s link structure ($W^T \mathbf{r}$) and the initial relevance encoded in the personalization vector \mathbf{v} [6].

The resulting score for each node reflects its overall importance, factoring in both its direct relevance to the input image and its semantic connections to other high-quality items. This process effectively promotes a coherent and representative subset of information. Finally, we use the PageRank scores to select the top- k captions and top- N few-shot examples to construct the final prompt, ensuring it is both concise and contextually rich, thereby enhancing the quality of the generated captions. An illustration of the application of PageRank, and the change of node values from SigLIP similarity to final PageRank scores, is given in Figure 2.

D. Prompting for Caption Generation

The retrieved and re-ranked information is formatted into a textual prompt for a language model with multilingual capabilities. Compared to the prompt used in the original LMCap approach [2], we adopt a more explicit formulation of the captioning task objective, structured in four main sections. Depending on the strategy being adopted, the prompt is either

fed to a text-only multilingual LLM, or to a multimodal VLM. The same overall structure is used across both strategies, allowing for a more controlled comparison between the two. The differences between them are minimal and localized, as illustrated in Figure 3.

First, we include a paragraph containing clear instructions regarding the task that we aim the model to perform, and describing the input that will be provided in the following sections. Second, the prompt includes a set of few-shot examples composed by retrieved captions for images similar to the input, illustrating how the captioning task should be performed. Third, we list the retrieved captions for the input image. Finally, the fourth section contains some additional instructions to further guide the model in processing all the information previously presented, and asking the model to generate the final caption. The model uses all this information to generate the final caption in the target language in a few-shot setting, meaning that we do not require any training (i.e., the captions are generated by providing information in the prompt, at inference time, to the language model).

To ensure that the final prompt remains free of duplicated captions, we apply a filtering procedure using the PageRank-based re-ranked elements. For each input image, the algorithm explores combinations of k retrieved captions drawn from its top-10 candidates, according to the PageRank score hierarchy, giving priority to those with higher scores. These selected captions are marked as used, and for each of the top-10 re-ranked most similar images, the algorithm selects the first unused gold caption as a candidate. It then verifies whether a complete set of N few-shot examples can be formed without redundancy. For each gold candidate, the few-shot retrieved captions are filtered against a dynamic mask containing all previously and potentially used captions. If at least k unique captions remain, the top- k are kept. The procedure stops as soon as a full, repetition-free prompt is successfully built, ensuring that all included captions and examples correspond to the highest-ranking PageRank scores.

IV. EXPERIMENTAL SETUP

This section summarizes the experimental configuration used in all evaluations. Unless otherwise noted, we set $N = k = 3$ (i.e., three few-shot examples and three retrieved captions per example and for the input image).

For graph-based re-ranking, we use the implementation of personalized PageRank from NetworkX [29] with damping $\alpha = 0.9$, i.e. at each iteration there is a 90% chance of following edges in the multimodal graph (propagating semantic relevance), and a 10% chance of teleporting to nodes according to the personalization vector, which biases the process toward considering the similarity to the input image.

In addition to our main experimental configuration (with PageRank and the Large Language Models described below), we also report on a set of additional experiments: (i) an experiment with a generalist visual encoder, not fine-tuned to the remote sensing domain; (ii) an ablation without PageRank re-ranking; and (iii) an experiment without the use of retrieved captions and few-shot examples, for the VLM setup. Image

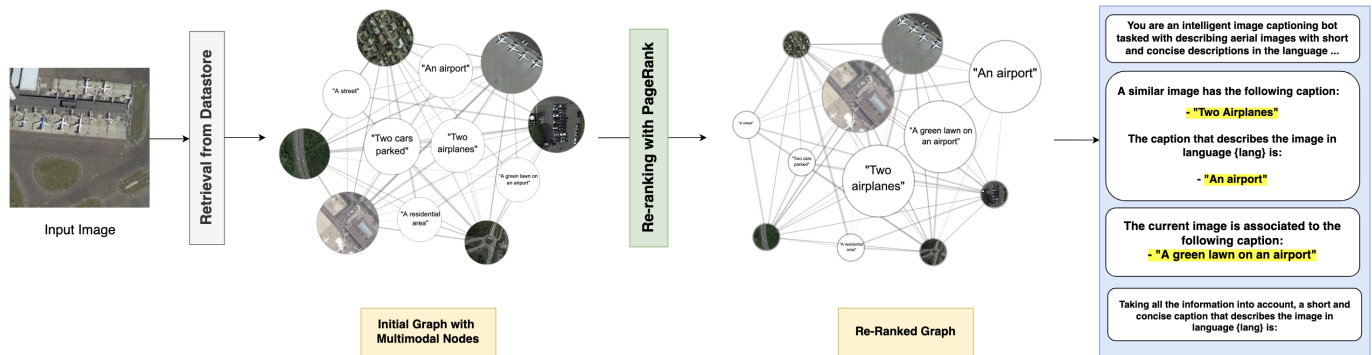


Fig. 2: An illustration for how the PageRank algorithm influences the final composition of the prompt. On the left, the weighting of the elements is based solely on SigLIP similarities (i.e., the original ranking). On the right, after PageRank propagation, the elements are re-ranked into a different distribution of node weights. For simplicity, this representation considers fewer elements and final retrieved captions compared to the experiments reported in the paper.

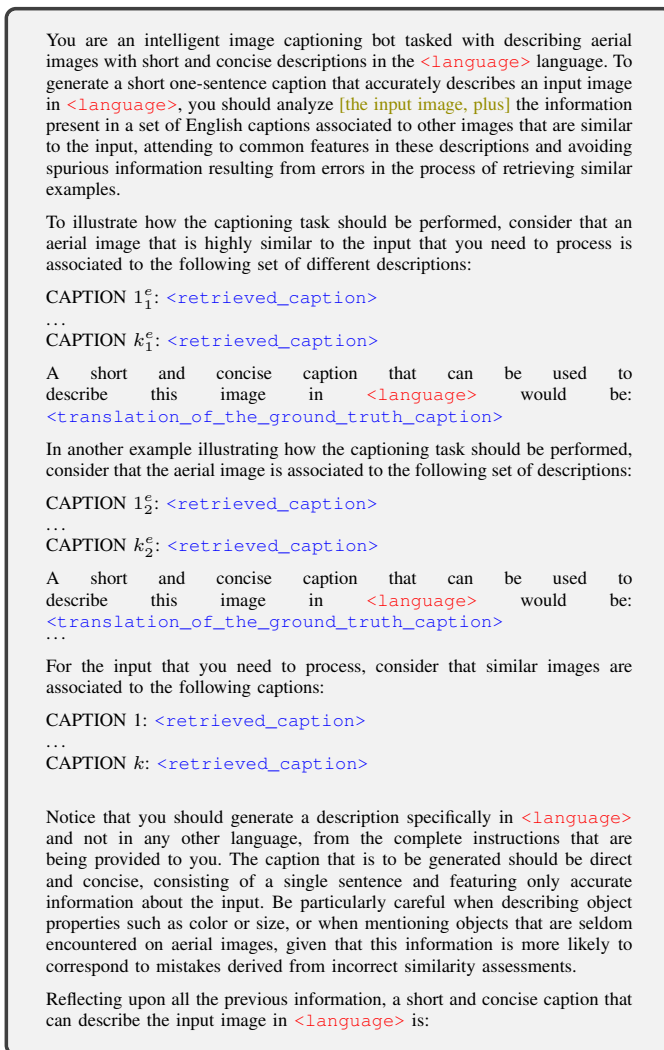


Fig. 3: Prompt for image captioning from the retrieved results. The green text between brackets corresponds to the changes made when using the image-aware strategy, in order to take into account the input image.

captioning performance was evaluated with standard metrics from the COCOeval package¹ with SacreBLEU tokenization², namely through the BLEU1, BLEU4, and CIDEr evaluation metrics, and also with a RefCLIPScore variant [30], that uses the RS-SigLIP2 encoder, which we called RefSigLIPScore, and that assesses similarities between the generated caption and (a) the input image plus (b) the ground-truth English caption. The following subsections detail the visual encoder, language models, and datasets that were used.

A. SigLIP2 Visual Encoder and Domain-Specific Fine-Tuning

We adopt SigLIP2 [4] as visual encoder and retrieval model, using a model derived from the *siglip2-large-patch16-256*³ version. We choose the large variant for its higher representational capacity and stronger alignment performance.

We specifically used a SigLIP2 model that was fine-tuned to the remote sensing domain (RS-SigLIP2) using the same English datasets and training procedure described in connection to RS-M-CLIP [10]. The training objective combines (i) a contrastive alignment loss to encourage cross-modal matching, and (ii) self-distillation on the image encoder (based on DINO [31]), where a student matches a teacher updated via Exponential Moving Average (EMA) under diverse augmentations. The final loss averages the alignment and self-distillation terms.

B. Language Models and Decoding Setup

In the image-blind variant, the prompt shown in Figure 3 is fed to a multilingual LLM. We tested the following four different multilingual language models:

- **TowerInstruct-7B-v0.2**⁴ [32]: A 7B parameter model that is efficient and fluent for multilingual generation model, instruction-tuned and supporting 10 languages.

¹<https://github.com/salaniz/pycocoevalcap>

²<https://github.com/mjpost/sacrebleu>

³<https://huggingface.co/google/siglip2-large-patch16-256>

⁴<https://huggingface.co/Unbabel/TowerInstruct-7B-v0.2>

TABLE I: Statistical characterization of the different remote sensing image captioning datasets used in our experiments.

Dataset	#Classes	#Images	Size	Resolution	#Captions
NWPU-Captions [20]	45	31,500	256 × 256	approx. 30–0.2m	157,500
RSICD [36]	30	10,921	224 × 224	var. resolutions	54,605
Sydney-Captions [37]	7	613	500 × 500	0.5m	3,065
UCM-Captions [37]	21	2,100	256 × 256	approx. 0.3m	10,500

- **EuroLLM-9B/22B-Instruct**^{5,6} [33]: Instruction-tuned multilingual models targeting high-quality generation across European and globally relevant languages. We use both the 9B and 22B variants to assess scaling effects.
- **Gemma3-12B-it**⁷ [34]: A recent multilingual instruction-tuned model with strong performance in cross-lingual generation and instruction following.

For efficiency, all LLMs are served via HuggingFace Transformers [35] with 4-bit quantization (bitsandbytes NF4), which substantially reduces memory usage without significantly degrading the generation quality.

For the image-aware variant, we use **EuroVLM-9B**⁸, which augments EuroLLM-9B with a visual encoder based on a SigLIP/SigLIP2-style ViT, and **Gemma3-12B-it** in its VLM configuration. In both cases, visual embeddings are projected into the text latent space and concatenated to the prompt, enabling joint attention over visual and textual context.

Caption generation uses deterministic beam search with a beam width of 3, offering stable and reproducible outputs aligned with the prompt content, which is desirable for automatic metrics (e.g., BLEU, CIDEr) that reward exact n -gram matches, while avoiding variance from stochasticity.

C. Remote Sensing Datasets

The remote sensing image captioning datasets that were used in our experiments are described next and also summarized in Table I.

- RSICD features a large set of images collected from different sources [36]. The images were manually annotated with short captions, but many of the captions are duplicated to ensure 5 captions per image;
- UCM-Captions and Sydney-Captions are based on two popular remote sensing scene classification datasets that were repurposed for image captioning by manual annotation [37]. Although extensively used, these datasets are small and have limitations in the fact that the captions correspond to very simple sentences that are highly similar between themselves;
- NWPU-Captions is currently the largest dataset of images paired to short captions in the remote sensing domain [20]. Each image is associated to 5 manually annotated captions, and the images span over a large set of classes, describing different land coverage types.

The training split of the aforementioned datasets was used to build the common datastore from which we retrieve the similar captions and the few-shot examples.

⁵<https://huggingface.co/utter-project/EuroLLM-9B-Instruct>

⁶<https://huggingface.co/utter-project/EuroLLM-22B-Instruct-Preview>

⁷<https://huggingface.co/google/gemma-3-12b-it>

⁸<https://huggingface.co/utter-project/EuroVLM-9B-Preview>

To evaluate captioning performance in different languages, and given the current lack of multilingual datasets for the task of remote sensing image captioning, we translated the captions from the test set instances of all four aforementioned datasets. We used a larger TowerInstruct-13B⁹ language model [32], whose fine-tuning strategy had a specific focus on machine translation tasks, and which has state-of-the-art performance in several high-resource languages. Given that captions for remote sensing images are often relatively simple sentences, automatic machine translation should not introduce significant errors, thus corresponding to a simple and effective approach that allows us to test multilingual image captioning methods in the remote sensing domain.

The TowerInstruct-13B model was prompted in a zero-shot manner to translate the individual English captions into the nine other languages that are supported by the model, namely German, French, Spanish, Chinese, Portuguese, Italian, Russian, Korean, and Dutch. The following instruction was used to perform the translation of the captions: “Translate the following text from English into {language}.\nEnglish: {caption}\n{language}:”

In the proposed method, the few-shot examples are collected with basis on image retrieval, but consist of retrieved English captions together with a ground-truth caption in the target language. The same machine translation approach was used to obtain these translated ground-truth captions.

Note also that, instead of directly producing captions in a target language, we could also consider generating captions in English, afterwards using the same TowerInstruct model to perform the translation to the target language. However, by directly generating captions in the target language, we avoid this second translation step at inference time, and we can better leverage the capabilities of language models that support a more extensive set of languages. We nonetheless report on an experiment in which we use this two-step generate-then-translate approach, showing that our method performs better.

V. RESULTS AND DISCUSSION

This section presents the experimental results obtained with the proposed approach and discusses the contribution of each component to the overall performance. We begin by reporting the main results, where our method is evaluated against existing state-of-the-art models, using the complete pipeline described in the previous sections (Section V-A). Next, we conduct several additional experiments to assess the robustness and design choices of the approach. First, we analyze the effect of using a generic visual encoder instead of the fine-tuned one, to isolate the impact of visual adaptation (Section V-B). Then, we perform an ablation study where the PageRank-based re-ranking step is removed, allowing us to quantify the gains introduced by this algorithm (Section V-C1). We also study the impact of varying the number of retrieved captions (k) and few-shot examples (N) (Section V-C2). Finally, we investigate the influence of the retrieved content on both the prompt composition and the caption generation process, providing a

⁹<https://huggingface.co/Unbabel/TowerInstruct-13B-v0.1>

TABLE II: Performance for both the image-blind (LLMs) and image-aware (VLMs) versions, across the four datasets. In the second part of the table, we provide English captioning results, as reported in prior work involving supervised learning. The best English results are in bold, and the best multilingual results are underlined.

Model	RSICD			UCM			Sydney			NWPU		
	BLEU1	BLEU4	CIDEr									
TowerInstruct-7B (EN)	0.607	0.249	0.567	0.882	0.723	3.462	0.778	0.574	2.392	0.842	0.582	1.573
TowerInstruct-7B (AVG)	0.556	0.207	0.542	0.812	<u>0.598</u>	<u>2.389</u>	0.712	<u>0.487</u>	<u>1.642</u>	0.773	<u>0.503</u>	<u>1.223</u>
EuroLLM-9B (EN)	0.646	0.283	0.678	0.875	0.699	3.374	0.805	0.579	2.315	0.855	0.561	1.503
EuroLLM-9B (AVG)	0.558	0.212	0.560	0.813	0.591	2.327	0.722	0.483	1.504	0.762	0.469	1.091
Gemma3-12B-LM (EN)	0.632	0.256	0.691	0.867	0.681	3.170	0.774	0.521	2.050	0.866	0.516	1.403
Gemma3-12B-LM (AVG)	<u>0.574</u>	<u>0.214</u>	<u>0.576</u>	<u>0.821</u>	0.549	2.131	0.738	0.460	1.426	<u>0.796</u>	0.427	1.011
EuroLLM-22B (EN)	0.645	0.259	0.780	0.840	0.619	3.080	0.763	0.494	1.860	0.804	0.473	1.247
EuroLLM-22B (AVG)	0.565	0.199	0.536	0.804	0.546	2.206	0.714	0.457	1.399	0.748	0.401	0.939
EuroVLM-9B (EN)	0.571	0.213	0.605	0.870	0.687	3.435	0.768	0.555	2.295	0.788	0.479	1.321
EuroVLM-9B (AVG)	0.547	0.190	0.525	0.812	0.578	2.369	0.705	0.462	1.540	0.748	0.433	1.033
Gemma3-12B-VLM (EN)	0.613	0.245	0.578	0.879	0.697	3.221	0.769	0.531	2.066	0.851	0.505	1.351
Gemma3-12B-VLM (AVG)	0.562	0.194	0.531	0.811	0.535	2.034	<u>0.741</u>	0.462	1.383	0.774	0.384	0.925
MLCA-NET [20]	0.757	0.461	2.356	0.826	0.668	3.240	0.831	0.580	2.324	0.745	0.478	1.164
HCNet [21]	–	–	–	0.883	0.745	3.518	0.769	0.610	2.471	0.896	0.717	2.093
MC-Net [22]	0.728	0.433	2.454	0.845	0.679	3.355	0.834	0.607	2.564	0.741	0.478	1.159
BITA [23]	0.774	0.504	3.054	0.889	0.719	3.845	–	–	–	0.885	0.676	1.970
Aware-Transform [24]	–	–	–	0.901	0.781	3.779	0.854	0.651	2.832	0.915	0.750	2.147
Def. Transform [25]	0.758	0.492	2.581	0.823	0.679	3.463	0.837	0.666	3.037	0.752	0.483	1.207
RSGPT [14]	0.703	0.368	1.029	0.861	0.657	3.332	0.823	0.622	2.731	–	–	–
SkyEyeGPT [16]	0.867	0.600	0.837	0.907	0.784	2.368	0.919	0.774	1.811	–	–	–

deeper understanding of how external information contributes to model performance (Section V-C3).

A. Main Evaluation Results

We first report results obtained with the proposed approach across the aforementioned four remote sensing datasets, comparing the image-blind (LLMs) and image-aware (VLMs) variants. Performance is measured with BLEU-1, BLEU-4, and CIDEr, considering both English captions and the average results across nine other languages (Portuguese, Spanish, French, German, Dutch, Italian, Chinese, Korean, and Russian).

Table II presents the complete results, comparing our models against state-of-the-art approaches from the literature. The results show that TowerInstruct-7B and Gemma3-12B-LM lead to very competitive training-free models, consistently achieving high scores across datasets and languages. EuroLLM-9B also performs strongly, while its larger 22B counterpart underperforms in most cases, showing that parameter scaling does not guarantee better performance in this setup. As expected, multilingual averages are lower than English results, reflecting variability across target languages. Surprisingly, vision-language models achieve slightly lower scores than the text-only LLM counterparts, which suggests that these models generate captions that do not exactly match the style that is used in the considered remote sensing datasets, and that current lexical-overlap metrics may fail to capture the benefits of including image inputs. Importantly, when compared with existing domain-specific large vision and language models, or fully supervised encoder-decoder models, our training-free models remain competitive, matching or surpassing some systems in BLEU and CIDEr, particularly on the UCM, Sydney, and NWPU datasets.

Since n -gram based evaluation metrics focus on surface overlap, they may undervalue captions that are lexically diverse or paraphrastic, but semantically correct. To address this, we additionally report RefSigLIPScores, shown in Table III. As opposed to BLEU and CIDEr metrics, RefSigLIPScore has not been used before in benchmarks, but it is still useful to understand the alignment between captions and input images. Results indicate that semantic grounding remains stable across models, with the larger LLM, i.e. EuroLLM-22B, often achieving scores comparable to or higher than smaller models, even in cases where n -gram metrics decline. This reveals that the choice of evaluation metric plays a crucial role, and we can either analyse the outputs by comparing them with reference captions in terms of how many n -grams are matched, or by assessing whether the generated caption is semantically aligned with the image itself.

In order to illustrate how the proposed method worked, and the outputs produced by different models, an example for the results is given in Figure 4. One can observe the importance of the captions chosen for the prompt, which the models end up using as basis for their generation. This includes not only the retrieved captions for the input image, but also the few-shot examples as well.

One of the key findings from our results is the performance gap across datasets, with RSICD consistently having the lowest scores across all models. Since this dataset systematically underperforms under our strategy, it is crucial to identify what distinguishes it from the others. To this end, we analyzed the overlap between the n -grams appearing in the prompt captions and those in the ground-truth references. A lower overlap implies that the prompt is less informative, providing weaker guidance for the model.

For each input image, the sets of unique 1-grams and 4-

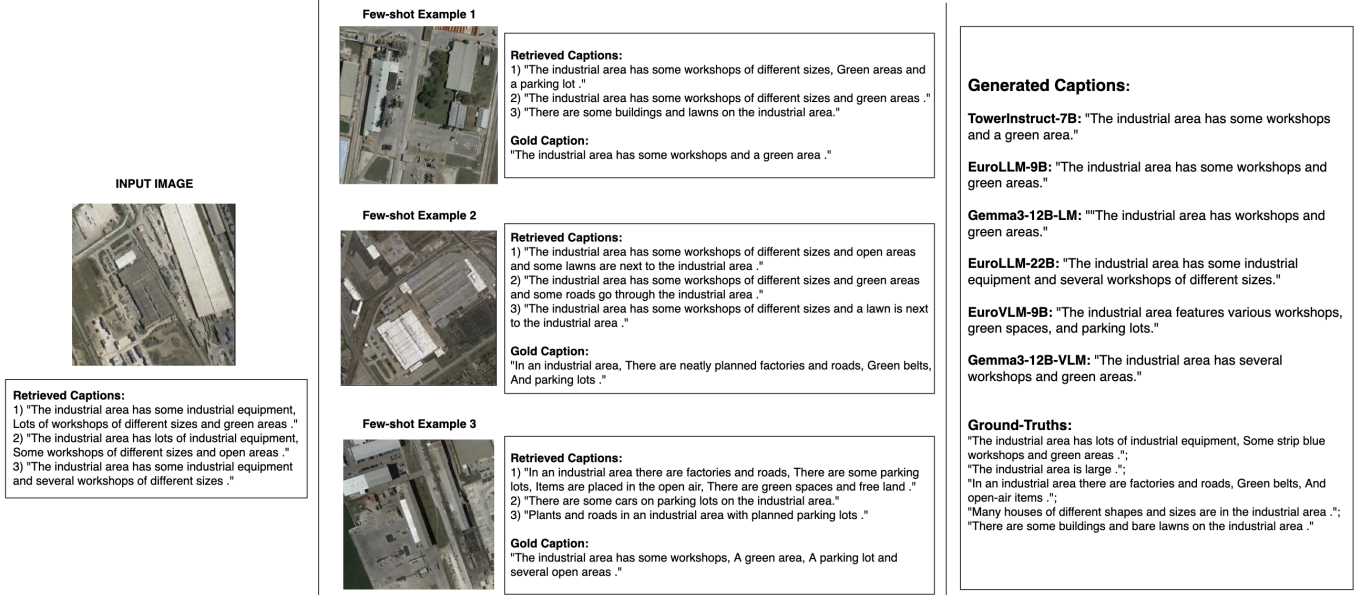


Fig. 4: Examples of generated captions from our models, for the English language and using the input image, the retrieved captions for the input image, and the few-shot examples, with re-ranking through personalized PageRank.

TABLE III: Mean RefSigLIPScore values for each model and dataset, reported for English (EN) and for the average across 9 languages (AVG). The best English results are in bold, and the best multilingual results are underlined.

Model	RefSigLIPScore			
	RSICD	UCM	Sydney	NWPU
TowerInstruct-7B (EN)	0.209	0.362	0.359	0.368
TowerInstruct-7B (AVG)	0.251	0.377	0.376	0.379
EuroLLM-9B (EN)	0.231	0.361	0.365	0.367
EuroLLM-9B (AVG)	0.266	<u>0.378</u>	0.377	0.381
Gemma-12B-LM (EN)	0.228	0.359	0.349	0.338
Gemma-12B-LM (AVG)	<u>0.274</u>	0.375	0.374	0.380
EuroLLM-22B (EN)	0.258	0.351	0.367	0.365
EuroLLM-22B (AVG)	0.267	0.377	<u>0.379</u>	<u>0.383</u>
EuroVLM-9B (EN)	0.225	0.360	0.360	0.351
EuroVLM-9B (AVG)	0.254	0.373	0.373	0.372
Gemma-12B-VLM (EN)	0.220	0.355	0.356	0.337
Gemma-12B-VLM (AVG)	0.267	0.366	0.370	0.368

grams were extracted from the prompt captions and compared with those from the five reference captions. Overlap was quantified using precision and recall, defined as $P(A, B) = \frac{A \cap B}{A}$ and $R(A, B) = \frac{A \cap B}{B}$, where A denotes the set of prompt n -grams and B the set of reference n -grams. Mean results for each dataset are given in Table IV, and they show that RSICD exhibits substantially lower precision and recall compared to the other datasets, indicating weaker prompt-reference alignment. Combined with the fact that only 5% of RSICD images contain five distinct reference captions, this explains the poorer performance of our strategy. The prompts are less aligned and coherent, and consequently the generated captions align less effectively with the references.

TABLE IV: Prompt-reference overlap (in percentage) using precision and recall metrics, for the four datasets. For each part of the prompt, the 1-gram and 4-gram overlap was computed considering every single caption in the prompt.

Dataset	Precision		Recall	
	1-gram	4-gram	1-gram	4-gram
RSICD	38%	5%	60%	13%
UCM	60%	27%	89%	64%
Sydney	58%	21%	85%	48%
NWPU	60%	21%	76%	45%

Another relevant aspect of our strategy is the performance gap between VLMs and their text-only LLM counterparts. Overall, LLM versions tend to achieve better results, with Gemma3 being the model where the two versions are most comparable. The key difference is that VLMs have access to the image, allowing them to introduce image-specific content that would not be inferred from the prompt alone. While this can enrich the generated captions, it also reduces the influence of the prompt. Since the prompt content is generally well aligned with the references, weaker reliance on it often leads to the generation of n -grams that are misaligned with both the prompt and the references, ultimately degrading performance.

Table V reports the distribution of generated 1-grams, occurring or not within the ground-truth references, further segmented by whether they were present in the prompt or not. The results confirm this effect, with VLMs generating more valid 1-grams not included in the prompt, but also producing a substantially higher number of invalid n -grams absent from the prompt. This negatively impacts BLEU and CIDEr scores. However, because the generated content still remains visually consistent with the image, the RefSigLIPScore is not

TABLE V: Valid and invalid 1-grams present or absent in the captions of the prompt, for both the LLM and VLM versions of the models that were used.

Dataset	Model	In-prompt		Not In-prompt	
		Valid 1-grams	Invalid 1-grams	Valid 1-grams	Invalid 1-grams
RSICD	EuroLLM-9B	7857	3290	10	898
	EuroVLM-9B	7927	3719	101	2124
	Gemma3-12B-LM	7232	2615	26	776
	Gemma3-12B-VLM	7078	2665	43	1294
UCM	EuroLLM-9B	1977	253	2	14
	EuroVLM-9B	2095	268	0	31
	Gemma3-12B-LM	1888	212	1	30
	Gemma3-12B-VLM	1940	217	3	24
Sydney	EuroLLM-9B	603	142	0	2
	EuroVLM-9B	627	174	0	9
	Gemma3-12B-LM	548	142	0	11
	Gemma3-12B-VLM	560	141	0	18
NWPU	EuroLLM-9B	33886	5150	27	174
	EuroVLM-9B	34046	6186	147	2257
	Gemma3-12B-LM	29414	3654	57	700
	Gemma3-12B-VLM	29972	3944	100	1059

VLM Positive Influence		
	<p>Gemma3-12B-LM</p> <p>Several airplanes are parked on the runway near a building.</p>	<p>BLEU1: 0.664 BLEU4: 0.381 CIDEr: 0.508</p>
	<p>Gemma3-12B-VLM</p> <p>Three airplanes are parked on the runway near a building.</p>	<p>BLEU1: 0.747 BLEU4: 0.392 CIDEr: 0.821</p>
VLM Negative Influence		
	<p>Gemma3-12B-LM</p> <p>Many green rectangular farmlands of different sizes are visible.</p>	<p>BLEU1: 0.900 BLEU4: 0.680 CIDEr: 1.750</p>
	<p>Gemma3-12B-VLM</p> <p>Many tan, dark green and light green mixed rectangular farms of different sizes and shapes.</p>	<p>BLEU1: 0.647 BLEU4: 0.219 CIDEr: 0.598</p>

Fig. 5: Example for the positive and negative effects of using VLMs. On the first case, the input image helps the model clarifying that there are "three" airplanes on the photo, being rewarded by the references. On the other hand, on the second case, the VLM describes in too much detail the image, becoming less aligned with references and having lower scores.

significantly affected. Additionally, these results show that the prompt is the key driver of generation for both VLMs and LLMs, because the majority of the valid (and invalid) 1-grams that are generated are present in the prompt, which translates into a large influence of the prompt on the final generation, independently of having the input image present or not. An example of both the positive or negative influence of using the VLM and the input image, together with the textual prompt, is represented in Figure 5.

Finally, we present in detail the multilingual results for one of our models, namely Gemma3-12B-LM, in Table VI. Our strategy shows similar performance across languages, with the notable exception of Russian, which performs consistently worse on n -gram-based metrics. However, the RefSigLIP-Score values are comparable to other languages, suggesting some inconsistencies in evaluation.

An illustrative example of the multilingual performance of Gemma3-12B-LM, with three different target languages and the English ground-truth, is presented in Figure 6.

Image	Gold Caption	English	Portuguese	German
	A plane is on the runway next to the grass.	A plane is parked on the runway next to the grass .	Um avião está na pista ao lado da relva.	Ein Flugzeug befindet sich auf der Landebahn neben dem Gras.
	The yellow island is surrounded by green water .	The island has some farmland and is surrounded by green waters.	A ilha central tem algumas terras agrícolas e a cor do rio é verde.	Die zentrale Insel hat einige landwirtschaftliche Flächen und ist von grünem Wasser umgeben.
	The sparse residential is on the grass next to some trees .	In a sparse residential area there are many trees.	Numa área residencial escassa, há muitas árvores verdes.	In einem dünn besiedelten Wohngebiet befinden sich viele grüne Bäume.

Fig. 6: Examples of captions generated with the Gemma3-12B large language model, with the complete method and for three different languages.

One of the reasons for adopting the proposed strategy, instead of generating English captions and translating them into the target language, is that translation introduces an additional computational step and error sources that can degrade caption quality, particularly for n -gram-based evaluation metrics. To assess this, we tested a generate-then-translate strategy, applying the same translation procedure to both the generated captions and to the ground-truth. Results are given in Table VII, showing identical RefSigLIPScore values, as expected since this metric evaluates image-caption alignment and is less sensitive to translation noise. However, BLEU and CIDEr scores are consistently lower under translation, confirming the drawbacks of this approach.

For future work, it would be valuable to build multilingual datasets with human-annotated references, enabling more reliable evaluations and stronger comparisons with alternative image captioning strategies.

B. Impact of Fine-tuning the Visual Encoder

Following the experiments presented earlier, we further investigated the impact of using RS-SigLIP2 as the visual encoder, since in our main setup this model was fine-tuned with the domain data. To better understand the contribution of fine-tuning, we designed a comparable setup where retrieval was performed using the original SigLIP2 model, without any domain-specific fine-tuning. The results of this comparison are shown in Table VIII.

Overall, the non-fine-tuned setup exhibits systematically lower performance, which is consistent with expectations. Fine-tuning adapts the visual encoder to the remote sensing domain, allowing it to identify captions that more accurately match each target image in the datastore. This improvement propagates through the different steps in the proposed approach, as higher-quality retrieval leads to stronger prompts, which in turn guide the generation process more effectively. To confirm this effect, we performed a prompt-reference overlap analysis, similar to that described in the previous section. The results, presented in Table IX, show that the fine-tuned encoder achieves higher precision and recall than the non-fine-tuned encoder. In contrast, the lack of fine-tuning produces prompts

TABLE VI: Multilingual performance of the Gemma3-12B-LM model across datasets. Best results are highlighted in bold.

Language	RSICD				UCM				Sydney				NWPU			
	BLEU1	BLEU4	CIDEr	SigLIP												
English	0.632	0.256	0.691	0.228	0.867	0.681	3.170	0.359	0.774	0.521	2.050	0.349	0.866	0.516	1.403	0.338
Portuguese	0.582	0.223	0.628	0.266	0.823	0.567	2.392	0.377	0.751	0.496	1.577	0.376	0.797	0.438	1.131	0.380
Spanish	0.602	0.229	0.663	0.271	0.828	0.602	2.646	0.383	0.744	0.509	1.507	0.377	0.833	0.483	1.231	0.381
French	0.561	0.218	0.611	0.265	0.836	0.595	2.272	0.374	0.746	0.500	1.335	0.370	0.803	0.447	1.035	0.377
German	0.545	0.204	0.467	0.279	0.832	0.529	2.016	0.374	0.741	0.414	1.446	0.366	0.771	0.387	0.859	0.380
Dutch	0.591	0.207	0.564	0.269	0.832	0.528	2.072	0.372	0.785	0.493	1.504	0.368	0.820	0.427	1.039	0.382
Italian	0.571	0.217	0.586	0.273	0.828	0.581	2.416	0.376	0.693	0.467	1.507	0.372	0.771	0.393	0.963	0.380
Korean	0.670	0.270	0.644	0.278	0.823	0.523	1.697	0.357	0.748	0.495	1.600	0.373	0.844	0.490	1.076	0.381
Chinese	0.600	0.238	0.731	0.290	0.826	0.583	2.171	0.380	0.783	0.480	1.509	0.386	0.838	0.480	1.205	0.386
Russian	0.448	0.118	0.292	0.273	0.758	0.431	1.496	0.382	0.653	0.285	0.847	0.378	0.688	0.301	0.562	0.377

TABLE VII: Comparison between multilingual generation and a generate-then-translate approach, across datasets and using the BLEU, CIDEr and RefSigLIPScore metrics. The results are the average of the nine target languages.

Language	RSICD				UCM				Sydney				NWPU			
	BLEU1	BLEU4	CIDEr	SigLIP	BLEU1	BLEU4	CIDEr	SigLIP	BLEU1	BLEU4	CIDEr	SigLIP	BLEU1	BLEU4	CIDEr	SigLIP
TowerInstruct-7B	0.556	0.207	0.542	0.251	0.812	0.598	2.389	0.377	0.712	0.487	1.642	0.376	0.773	0.503	1.223	0.379
TowerInstruct-7B w/ Translation	0.544	0.183	0.485	0.257	0.784	0.501	1.882	0.376	0.701	0.416	1.220	0.370	0.731	0.381	0.906	0.384
EuroLLM-9B	0.558	0.212	0.560	0.266	0.813	0.591	2.327	0.378	0.722	0.483	1.504	0.377	0.762	0.469	1.091	0.381
EuroLLM-9B w/ Translation	0.575	0.204	0.546	0.275	0.781	0.493	1.879	0.378	0.720	0.420	1.198	0.380	0.741	0.372	0.880	0.389
Gemma-12B-LM	0.574	0.214	0.576	0.274	0.821	0.549	2.131	0.375	0.738	0.460	1.426	0.374	0.796	0.427	1.011	0.380
Gemma-12B-LM w/ Translation	0.565	0.194	0.531	0.267	0.791	0.493	1.800	0.378	0.697	0.393	1.068	0.371	0.755	0.353	0.859	0.375
EuroLLM-22B	0.565	0.199	0.536	0.267	0.804	0.546	2.206	0.377	0.714	0.457	1.399	0.379	0.748	0.401	0.939	0.383
EuroLLM-22B w/ Translation	0.547	0.185	0.505	0.274	0.743	0.436	1.715	0.372	0.687	0.388	1.007	0.379	0.696	0.318	0.736	0.383
EuroVLM-9B	0.547	0.190	0.525	0.254	0.812	0.578	2.369	0.373	0.705	0.462	1.540	0.373	0.748	0.433	1.033	0.372
EuroVLM-9B w/ Translation	0.517	0.164	0.472	0.263	0.767	0.470	1.832	0.375	0.699	0.420	1.189	0.371	0.686	0.319	0.773	0.370
Gemma-12B-VLM	0.562	0.194	0.531	0.267	0.811	0.535	2.034	0.366	0.741	0.462	1.383	0.370	0.774	0.384	0.925	0.368
Gemma-12B-VLM w/ Translation	0.563	0.193	0.520	0.271	0.786	0.494	1.800	0.377	0.695	0.399	1.095	0.372	0.743	0.343	0.831	0.373

TABLE VIII: Experiments with a SigLIP2 model without fine-tuning for the remote sensing domain, for every language model that was tested on the main experiments.

Model	RSICD				UCM				Sydney				NWPU			
	BLEU1	BLEU4	CIDEr	SigLIP	BLEU1	BLEU4	CIDEr	SigLIP	BLEU1	BLEU4	CIDEr	SigLIP	BLEU1	BLEU4	CIDEr	SigLIP
TowerInstruct-7B (EN)	0.552	0.191	0.453	0.132	0.773	0.568	2.728	0.282	0.690	0.408	1.555	0.289	0.746	0.421	1.171	0.255
TowerInstruct-7B (AVG)	0.526	0.182	0.472	0.194	0.766	0.546	2.104	0.331	0.686	0.409	1.253	0.349	0.713	0.404	0.953	0.308
EuroLLM-9B (EN)	0.515	0.138	0.383	0.115	0.724	0.493	2.420	0.247	0.694	0.393	1.455	0.271	0.721	0.363	1.033	0.222
EuroLLM-9B (AVG)	0.500	0.163	0.426	0.173	0.738	0.499	1.955	0.300	0.678	0.390	1.138	0.323	0.708	0.376	0.886	0.284
Gemma3-12B-LM (EN)	0.537	0.147	0.515	0.155	0.734	0.485	2.272	0.247	0.694	0.371	1.180	0.235	0.776	0.371	1.044	0.207
Gemma3-12B-LM (AVG)	0.479	0.135	0.379	0.169	0.691	0.385	1.451	0.259	0.630	0.319	0.826	0.278	0.714	0.316	0.741	0.249
EuroLLM-22B (EN)	0.456	0.089	0.338	0.091	0.554	0.258	1.132	0.146	0.597	0.309	1.171	0.228	0.640	0.263	0.754	0.193
EuroLLM-22B (AVG)	0.465	0.111	0.333	0.132	0.614	0.324	1.161	0.217	0.615	0.301	0.846	0.262	0.633	0.268	0.643	0.243
EuroVLM-9B (EN)	0.441	0.108	0.354	0.138	0.667	0.426	2.142	0.241	0.644	0.387	1.710	0.314	0.671	0.319	0.934	0.240
EuroVLM-9B (AVG)	0.488	0.137	0.426	0.192	0.726	0.483	1.945	0.311	0.671	0.379	1.182	0.351	0.677	0.334	0.813	0.295
Gemma3-12B-VLM (EN)	0.529	0.163	0.440	0.153	0.736	0.481	2.251	0.250	0.687	0.410	1.363	0.261	0.772	0.370	1.051	0.223
Gemma3-12B-VLM (AVG)	0.476	0.124	0.365	0.178	0.682	0.362	1.300	0.260	0.650	0.337	0.861	0.281	0.702	0.292	0.703	0.256

that are less aligned with the references, which directly results in weaker caption generation and lower final performance.

TABLE IX: Prompt-reference overlap (%) for Fine-Tuned (FT) and Non Fine-Tuned (NFT) visual encoders, per dataset.

Dataset	1-gram Precision		4-gram Precision		1-gram Recall		4-gram Recall	
	FT	NFT	FT	NFT	FT	NFT	FT	NFT
RSICD	38%	27%	5%	2%	60%	61%	13%	8%
UCM	60%	30%	27%	10%	89%	82%	64%	41%
Sydney	58%	33%	21%	10%	85%	83%	48%	36%
NWPU	60%	43%	21%	10%	76%	73%	45%	27%

An additional aspect worth analyzing is the effect of this change on VLMs. One might initially expect these models to be more robust to poorer retrieval, since they have direct access to the input image. However, our results indicate otherwise. Despite having visual information available, VLMs still rely heavily on the textual prompt as the primary driver for text generation. The majority of the generated n -grams, whether

correct or incorrect, seem to originate from the prompt. Consequently, when prompt quality deteriorates due to poorer retrieval, VLMs experience a performance drop similar to that of LLMs. This reinforces the conclusion that, in our strategy, the prompt remains the key element for achieving strong performance, with fine-tuning of the visual encoder playing a decisive role in ensuring that the prompt is both informative and aligned with the references.

C. Ablation Experiments

1) *Impact of PageRank Re-ranking*: To assess the impact of PageRank re-ranking on our approach, we designed an alternative setup where this step was omitted. In this configuration, the order of retrieval was determined solely by the similarity scores from RS-SigLIP2, both for the retrieved captions and for the ordering of the few-shot examples. This setup was applied to both the LLM and VLM strategies in order to

TABLE X: Results for the ablation study focused on re-ranking with PageRank, for the two alternative approaches.

Model	PageRank	Language	RSICD				UCM				Sydney				NWPU			
			BLEU1	BLEU4	CIDEr	SigLIP	BLEU1	BLEU4	CIDEr	SigLIP	BLEU1	BLEU4	CIDEr	SigLIP	BLEU1	BLEU4	CIDEr	SigLIP
EuroLLM-9B	No	EN	0.622	0.237	0.606	0.220	0.859	0.668	3.221	0.353	0.764	0.473	1.798	0.345	0.843	0.520	1.431	0.343
		AVG	0.543	0.191	0.520	0.262	0.789	0.557	2.215	0.377	0.660	0.384	1.150	0.364	0.722	0.427	0.937	0.364
	Yes	EN	0.646	0.283	0.678	0.231	0.875	0.699	3.374	0.361	0.805	0.579	2.315	0.365	0.855	0.561	1.503	0.367
		AVG	0.558	0.212	0.560	0.266	0.813	0.591	2.327	0.378	0.722	0.483	1.504	0.377	0.762	0.469	1.091	0.381
EuroVLM-9B	No	EN	0.518	0.167	0.518	0.218	0.841	0.642	3.218	0.348	0.734	0.469	1.849	0.347	0.747	0.409	1.159	0.323
		AVG	0.513	0.160	0.466	0.251	0.781	0.533	2.205	0.368	0.677	0.401	1.286	0.364	0.709	0.363	0.884	0.351
	Yes	EN	0.571	0.213	0.605	0.225	0.870	0.687	3.435	0.360	0.768	0.555	2.295	0.360	0.788	0.479	1.321	0.351
		AVG	0.547	0.190	0.525	0.254	0.812	0.578	2.369	0.373	0.705	0.462	1.540	0.373	0.748	0.433	1.033	0.372
GemmaLM	No	EN	0.595	0.220	0.632	0.226	0.848	0.656	3.066	0.351	0.725	0.439	1.519	0.338	0.850	0.472	1.289	0.313
		AVG	0.546	0.185	0.531	0.269	0.800	0.529	2.023	0.373	0.697	0.382	1.082	0.365	0.776	0.383	0.915	0.365
	Yes	EN	0.632	0.256	0.691	0.228	0.867	0.681	3.170	0.359	0.774	0.521	2.050	0.349	0.866	0.516	1.403	0.338
		AVG	0.574	0.214	0.576	0.274	0.821	0.549	2.131	0.375	0.738	0.460	1.426	0.374	0.796	0.427	1.011	0.380
GemmaVLM	No	EN	0.591	0.211	0.554	0.216	0.858	0.669	3.116	0.349	0.747	0.459	1.710	0.354	0.838	0.465	1.265	0.316
		AVG	0.535	0.168	0.487	0.265	0.791	0.506	1.955	0.364	0.702	0.389	1.142	0.360	0.750	0.337	0.818	0.355
	Yes	EN	0.613	0.245	0.578	0.220	0.879	0.697	3.221	0.355	0.769	0.531	2.066	0.356	0.851	0.505	1.351	0.337
		AVG	0.562	0.194	0.531	0.267	0.811	0.535	2.034	0.366	0.741	0.462	1.383	0.370	0.774	0.384	0.925	0.368

TABLE XI: Prompt–reference overlap (%) for the PageRank (PR) and no PageRank (NPR) cases, per dataset.

Dataset	1–gram Precision		4–gram Precision		1–gram Recall		4–gram Recall	
	PR	NPR	PR	NPR	FT	NPR	PR	NPR
RSICD	38%	34%	5%	4%	60%	64%	13%	13%
UCM	60%	57%	27%	26%	89%	90%	64%	64%
Sydney	58%	55%	21%	19%	85%	85%	48%	45%
NWPU	60%	56%	21%	18%	76%	77%	45%	40%

examine whether the effect differed between the two variants. Results are summarized in Table X.

The results reveal that the inclusion of PageRank re-ranking provides a clear improvement, particularly in terms of n -gram–based metrics such as BLEU and CIDEr. This effect is analogous to what was observed in the previous section when comparing fine-tuned and non fine-tuned visual encoders. Ultimately, PageRank contributes significantly to the quality of the prompt content provided to the models.

A prompt–reference overlap analysis, shown in Table XI, further illustrates this behavior. PageRank improves alignment by selecting a more coherent ordering of the retrieved captions, leading to prompts that are more consistent with the references. As a result, the final performance lies between that of the main setup (with fine-tuned retrieval plus PageRank) and the non fine-tuned retrieval baseline. These findings confirm that PageRank re-ranking plays a central role as a fine-tuning mechanism for prompt construction, refining the retrieved content and enhancing overlap with the references. At the same time, its effectiveness relies on the strength of the underlying retrieval step, highlighting that both high-quality visual encoding and re-ranking are necessary to achieve optimal results.

A full example illustrating the impact of PageRank is given in Figure 7, where we can see that the re-ranking mechanism changes completely the few-shot examples, the retrieved captions, and consequently also the final output.

2) *Impact of the Number of Retrieved Captions and Few-shot Examples:* In our retrieval-augmented captioning framework, the number of retrieved captions (k) and the number of few-shot examples included in the prompt (N) jointly determine how much external semantic context is provided to the language model. In the main experiments, we adopted the configuration $N = k = 3$, which balances prompt length and

retrieval diversity. However, increasing the amount of retrieved information may further improve the model’s ability to align image content with relevant caption patterns, at the cost of a longer prompt and potentially higher redundancy.

To assess the sensitivity of the proposed method to these parameters, we extend the analysis to two additional configurations: $N = k = 4$ and $N = k = 5$. Evaluating these larger settings allows us to understand whether retrieval diversity and prompt density continue to translate into performance gains, or whether diminishing returns emerge as the prompt grows.

Table XII reports the results obtained with the three configurations ($N = k = 3, 4, 5$), across the image-blind and image-aware versions. The results indicate a consistent improvement in captioning performance as N and k increase, although one should also note that this comes with higher costs in terms of LLM processing. The observed trend suggests that enlarging both the retrieved caption set and the few-shot context provides the language model with a richer pool of semantic cues, which in turn enhances the relevance and grounding of the generated captions. To better understand the mechanism behind this improvement, we performed a prompt–reference overlap analysis.

Figure 8 presents the comparison of 1-gram precision and recall across the three configurations ($N = k = 3, 4, 5$). As expected, increasing the number of retrieved captions and few-shot examples leads to a decrease in precision, possibly due to the larger number of n -grams introduced into the prompt. However, this expansion also results in a clear and consistent increase in recall, showing that a greater proportion of reference n -grams is represented in the prompt.

This rise in recall provides a direct explanation for the performance gains observed in Table XII. By exposing the model to more reference-aligned lexical and semantic content, the prompt becomes more informative and better grounded, enabling the model to produce captions that more closely resemble the reference descriptions.

3) *Image-aware Approach Without Retrieved Information:* To assess the contribution of in-context learning to VLM performance, we conducted an additional experiment where models were prompted without retrieved captions or few-shot examples. This setup aimed to establish a baseline for the intrinsic captioning ability of the considered VLMs, isolating them from external guidance. The prompt, shown in Figure 9,

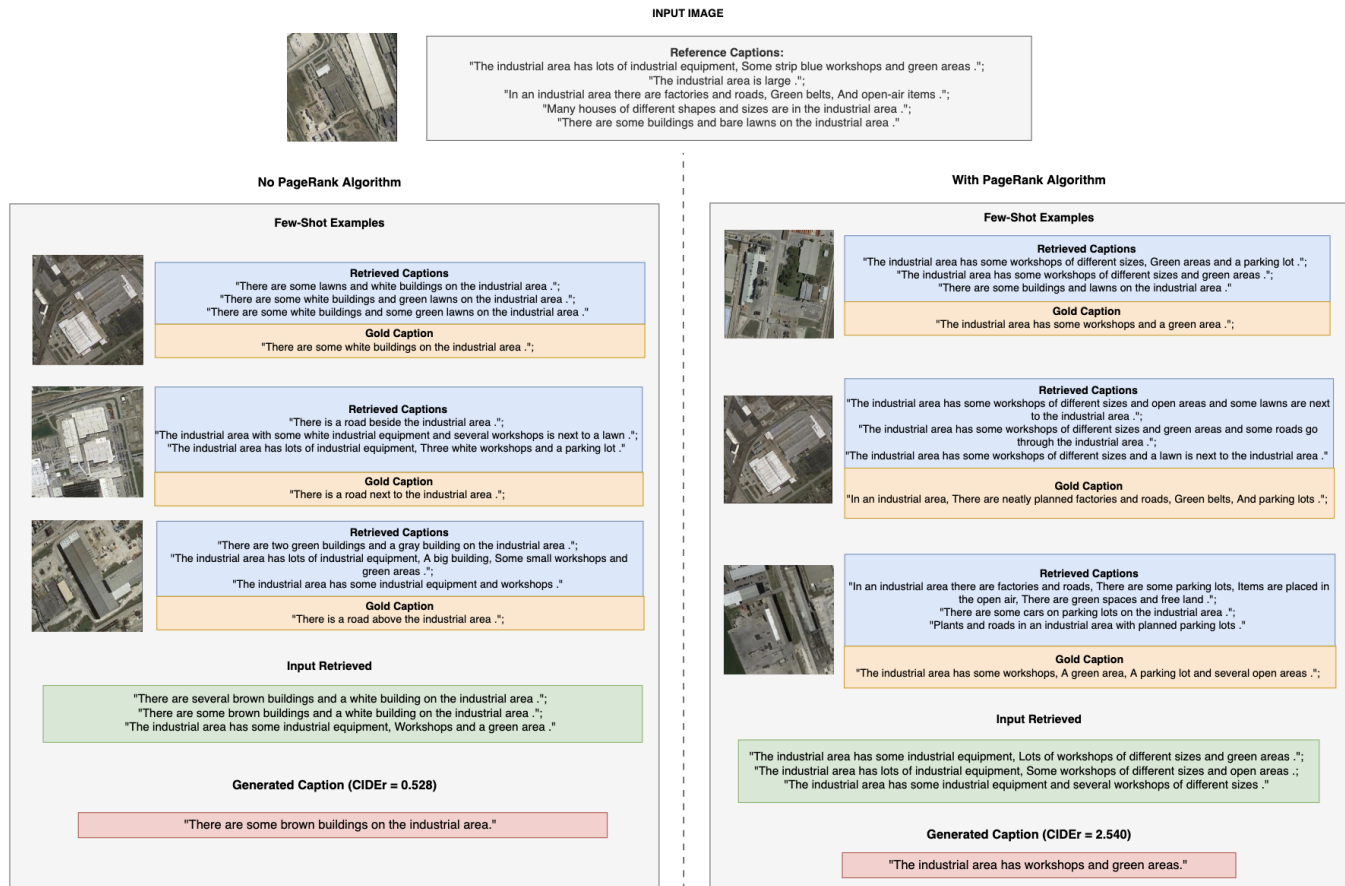


Fig. 7: Examples of prompts constructed with and without the use of the PageRank re-ranking algorithm, where the CIDEr score of the final generated caption has a very different value for the two cases.

TABLE XII: Results for the ablation study focused on varying the number of retrieved captions (k) and the number of few-shot examples (N), for the image-blind and image-aware approaches. For each model, the best English results are highlighted in bold, and the best multilingual results are underlined.

Model	N, k	Language	RSICD				UCM				Sydney				NWPU			
			BLEU1	BLEU4	CIDEr	SigLIP												
EuroLLM-9B	3	EN	0.646	0.283	0.678	0.231	0.875	0.699	3.374	0.361	0.365	0.855	0.561	1.503	0.367			
		AVG	0.558	0.212	0.560	<u>0.266</u>	<u>0.813</u>	0.591	<u>2.327</u>	<u>0.378</u>	0.722	0.483	<u>1.504</u>	0.377	0.762	0.469	1.091	<u>0.381</u>
	4	EN	0.652	0.286	0.697	0.233	0.884	0.706	3.448	0.361	0.785	0.564	2.212	0.364	0.859	0.572	1.537	0.366
		AVG	0.563	0.217	0.569	0.265	0.812	<u>0.594</u>	2.305	0.378	0.719	0.479	1.432	0.380	0.772	0.479	1.123	0.380
	5	EN	0.649	0.285	0.680	0.228	0.864	0.681	3.234	0.359	0.798	0.560	2.174	0.367	0.859	0.574	1.546	0.364
		AVG	<u>0.575</u>	<u>0.224</u>	<u>0.588</u>	<u>0.266</u>	0.801	0.583	2.286	0.376	<u>0.737</u>	<u>0.484</u>	1.408	0.378	<u>0.785</u>	<u>0.489</u>	<u>1.151</u>	0.379
EuroVLM-9B	3	EN	0.571	0.213	0.605	0.225	0.870	0.687	3.435	0.360	0.768	0.555	2.295	0.360	0.788	0.479	1.321	0.351
		AVG	0.547	0.190	0.525	0.254	0.812	0.578	<u>2.369</u>	0.373	<u>0.705</u>	<u>0.462</u>	<u>1.540</u>	0.373	0.748	0.433	1.033	0.372
	4	EN	0.596	0.227	0.675	0.237	0.873	0.691	3.446	0.360	0.761	0.555	2.294	0.357	0.808	0.509	1.388	0.356
		AVG	0.552	0.195	0.532	0.253	<u>0.813</u>	<u>0.579</u>	2.353	<u>0.374</u>	0.700	0.457	1.532	0.373	0.755	0.448	1.069	<u>0.373</u>
	5	EN	0.621	0.252	0.736	0.242	0.862	0.670	3.282	0.357	0.754	0.547	2.278	0.359	0.815	0.518	1.403	0.358
		AVG	<u>0.558</u>	<u>0.200</u>	<u>0.543</u>	<u>0.255</u>	0.801	0.563	2.265	0.373	<u>0.705</u>	0.460	1.493	<u>0.375</u>	<u>0.759</u>	<u>0.454</u>	<u>1.082</u>	<u>0.373</u>
GemmaLM	3	EN	0.632	0.256	0.691	0.228	0.867	0.681	3.170	0.359	0.774	0.521	2.050	0.349	0.866	0.516	1.403	0.338
		AVG	0.574	0.214	0.576	0.274	0.821	0.549	<u>2.131</u>	0.375	0.738	0.460	<u>1.426</u>	0.374	0.796	0.427	1.011	0.380
	4	EN	0.658	0.281	0.786	0.244	0.879	0.700	3.211	0.354	0.774	0.508	1.936	0.353	0.877	0.550	1.476	0.346
		AVG	0.590	0.228	0.607	0.276	<u>0.822</u>	<u>0.552</u>	2.064	<u>0.377</u>	0.744	0.465	1.348	<u>0.377</u>	0.805	0.445	1.058	<u>0.383</u>
	5	EN	0.669	0.290	0.856	0.254	0.872	0.696	3.215	0.353	0.806	0.576	2.186	0.359	0.882	0.571	1.523	0.349
		AVG	<u>0.593</u>	<u>0.229</u>	<u>0.616</u>	<u>0.278</u>	0.811	0.534	2.011	0.373	<u>0.752</u>	<u>0.470</u>	1.373	0.371	<u>0.811</u>	<u>0.455</u>	<u>1.081</u>	<u>0.383</u>
GemmaVLM	3	EN	0.613	0.245	0.578	0.220	0.879	0.697	3.221	0.355	0.769	0.531	2.066	0.356	0.851	0.505	1.351	0.337
		AVG	0.562	0.194	0.531	0.267	0.811	0.535	<u>2.034</u>	0.366	0.741	0.462	<u>1.383</u>	<u>0.370</u>	0.774	0.384	0.925	0.368
	4	EN	0.623	0.247	0.624	0.225	0.879	0.700	3.211	0.354	0.794	0.561	2.138	0.356	0.864	0.533	1.434	0.345
		AVG	0.568	0.203	0.550	0.268	<u>0.813</u>	<u>0.536</u>	1.975	<u>0.369</u>	0.743	<u>0.463</u>	1.330	<u>0.370</u>	0.787	0.404	0.974	0.374
	5	EN	0.637	0.261	0.689	0.235	0.872	0.696	3.215	0.353	0.797	0.578	2.181	0.352	0.871	0.554	1.476	0.349
		AVG	<u>0.575</u>	<u>0.207</u>	<u>0.561</u>	<u>0.271</u>	0.795	0.511	1.880	0.362	<u>0.754</u>	0.460	1.329	0.368	<u>0.795</u>	<u>0.415</u>	<u>0.997</u>	<u>0.375</u>

used the same initial instruction as the original, but excluded retrieved captions and few-shot examples.

Results in Table XIII show a consistent drop across all metrics, compared to the original strategy. Captions generated

TABLE XIII: Comparison on the use of VLMs with and without few-shot examples and retrieved captions.

Model	Retrieval	Lang	RSICD				UCM				Sydney				NWPU			
			BLEU1	BLEU4	CIDEr	SigLIP	BLEU1	BLEU4	CIDEr	SigLIP	BLEU1	BLEU4	CIDEr	SigLIP	BLEU1	BLEU4	CIDEr	SigLIP
EuroVLM	No	EN	0.324	0.027	0.084	0.154	0.293	0.043	0.198	0.132	0.233	0.015	0.051	0.108	0.371	0.029	0.102	0.125
	AVG	0.274	0.034	0.056	0.171	0.286	0.041	0.104	0.125	0.296	0.040	0.066	0.150	0.325	0.041	0.063	0.150	
EuroVLM	Yes	EN	0.571	0.213	0.605	0.225	0.870	0.687	3.435	0.360	0.768	0.555	2.295	0.360	0.788	0.479	1.321	0.351
	AVG	0.547	0.190	0.525	0.254	0.812	0.578	2.369	0.373	0.705	0.462	1.540	0.373	0.748	0.433	1.033	0.372	
GemmaVLM	No	EN	0.389	0.029	0.165	0.144	0.383	0.044	0.311	0.138	0.368	0.033	0.132	0.109	0.428	0.037	0.202	0.092
	AVG	0.345	0.039	0.124	0.153	0.348	0.052	0.205	0.127	0.375	0.050	0.106	0.138	0.392	0.043	0.134	0.142	
GemmaVLM	Yes	EN	0.613	0.245	0.578	0.220	0.879	0.697	3.221	0.355	0.769	0.531	2.066	0.356	0.851	0.505	1.351	0.337
	AVG	0.562	0.194	0.531	0.267	0.811	0.535	2.034	0.366	0.741	0.462	1.383	0.370	0.774	0.384	0.925	0.368	

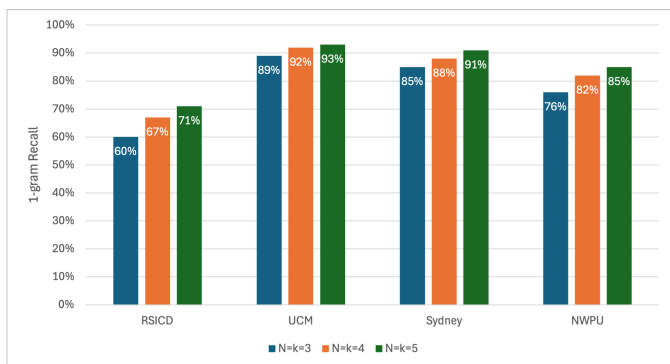
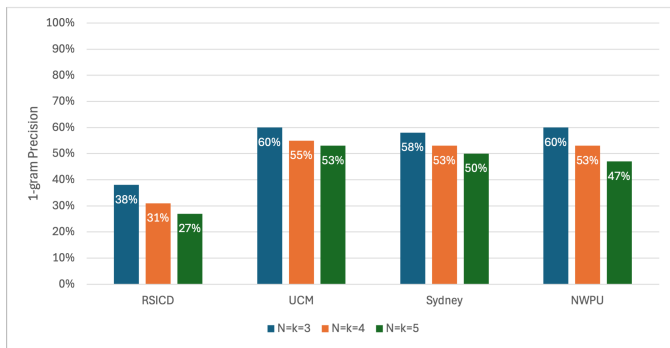


Fig. 8: Prompt-reference overlap (%) for the three N and k values that were considered ($N = k = 3, 4$ and 5). The top chart reports the 1-gram precision, and the bottom chart reports the 1-gram recall.

You are an intelligent image captioning bot tasked with describing aerial images with short and concise descriptions in the `<language>` language.

Notice that you should generate a description specifically in `<language>` and not in any other language. The caption that is to be generated should be direct and concise, consisting of a single sentence and featuring only accurate information about the input.

Reflecting upon all the previous information, a short and concise caption that can describe the input image in `<language>` is:

Fig. 9: Prompt given to the VLM for image captioning, without the use of retrieved captions or few-shot examples.

without in-context learning deviate from the expected style and structure, often omitting key details and failing to use terms that improve overlap with the ground-truth.

The decline in RefSigLIPScore values is especially notable. One might expect this metric to remain stable, since captions are generated with access to the input image. However, without

Image	Gold Caption	With Retrieval	Without Retrieval
	Two planes of different sizes are neatly parked next to the buildings in the airport .	Two planes of different sizes are parked next to the airport buildings.	Aerial view of airplanes parked at an airport terminal.
	The dark green river with a winding bank goes through the residential area .	The green river winds through the residential area.	Aerial view of a river winding through a densely populated area.

Fig. 10: Example illustrating the generated captions with the Gemma3-12B VLM, with and without few-shot examples and retrieved captions.

contextual examples, generalist VLMs produce captions that are stylistically and semantically misaligned with the remote sensing domain. Figure 10 illustrates this effect with a qualitative example from Gemma3-VLM, where captions without retrieval are simplified and less aligned than those from the original strategy.

VI. CONCLUSIONS

This work advanced the understanding of training-free multilingual captioning methods for remote sensing imagery, by systematically comparing different models in two settings, namely an image-blind approach where LLMs are prompted without access to the input image, and an image-aware approach where VLMs are guided by both textual instructions and the image itself.

We achieved competitive results against state-of-the-art approaches that include supervised training, with the results obtained with the TowerInstruct-7B and Gemma3-12B-LM models standing out in particular.

Performance was mostly consistent across datasets, with RSICD standing as the main exception. Its limited lexical diversity may explain a reduced prompt-reference alignment, leading to weaker outputs. Comparing the image-blind and image-aware setups further revealed that, while VLMs often underperform on n -gram-based quality metrics due to generating visually grounded but unseen tokens, they remain competitive under the RefSigLIPScore metric, confirming semantic alignment with the input image.

Another key achievement was the assessment of captioning performance in nine languages beyond English, with generally strong results, despite the lack of human-annotated multilingual datasets. Crucially, we validated that directly

prompting models in the target language yields better results than translating English captions post-hoc.

We also demonstrated the central role of retrieval quality. Fine-tuning the visual encoder significantly improved both caption selection and few-shot example matching, which translated into stronger prompt–reference alignment and higher-quality generations. The proposed PageRank-based re-ranking method further refined the retrieved content, boosting coherence and consistency with improvements of up to 35%.

Extending the analysis, we showed that increasing the number of retrieved captions and few-shot examples can further strengthen generation quality. Larger N and k values enriched the prompt with more reference-aligned lexical and semantic content, yielding measurable gains across models.

Finally, we evaluated a baseline where VLMs were prompted without retrieved captions or few-shot examples. Performance dropped sharply, underscoring the decisive role of retrieval and prompt design in shaping both the style and semantic accuracy of the generated captions.

Several promising directions also arise from our experimental findings. A key priority is the creation of human-annotated multilingual captioning datasets, which would enable more reliable evaluation and reduce the limitations of translation-based references. Exploring diverse multimodal encoders, with different architectures, also appears essential, given the central role of retrieval quality.

Finally, future research should investigate the use of advanced reasoning models [38], which may provide richer interpretative abilities (e.g., for assessing inconsistencies between all the retrieved information) and lead to the generation of more contextually accurate captions.

ACKNOWLEDGMENTS

This research was supported by the Portuguese Recovery and Resilience Plan through project C645008882-00000055 (i.e., the Center For Responsible AI), and also by the Fundação para a Ciência e Tecnologia (FCT), through the projects UIDB/50021/2020 and UIDP/04516/2020 (DOIs: [10.54499/UIDB/50021/2020](https://doi.org/10.54499/UIDB/50021/2020), [10.54499/UIDP/04516/2020](https://doi.org/10.54499/UIDP/04516/2020)).

REFERENCES

- [1] Y. Tewel, Y. Shalev, I. Schwartz, and L. Wolf, “ZeroCap: Zero-Shot Image-to-Text Generation for Visual-Semantic Arithmetic,” in *Proceedings of IEEE Conference on Computer Vision and Pattern Recognition*, 2022.
- [2] R. Ramos, D. Elliott, and B. Martins, “LMCap: Few-shot multilingual image captioning by retrieval-augmented prompting,” in *Findings of the ACL*, 2023.
- [3] T. Kim *et al.*, “NICE: CVPR 2023 challenge on zero-shot image captioning,” in *Proceedings of IEEE Conference on Computer Vision and Pattern Recognition*, 2024.
- [4] M. Tschannen *et al.*, “SigLIP2: Multilingual Vision-Language Encoders with Improved Semantic Understanding, Localization, and Dense Features,” 2025. [Online]. Available: <https://arxiv.org/abs/2502.14786>
- [5] L. Page, S. Brin, R. Motwani, and T. Winograd, “The PageRank Citation Ranking: Bringing Order to the Web,” Stanford InfoLab, Tech. Rep., 1999.
- [6] D. F. Gleich, “PageRank Beyond the Web,” *Society for Industrial and Applied Mathematics Review*, vol. 57, no. 3, 2015.
- [7] L. Bashmal, Y. Bazi, F. Melgani, M. M. Al Rahhal, and M. A. Al Zuair, “Language Integration in Remote Sensing: Tasks, datasets, and future directions,” *IEEE Geoscience and Remote Sensing Magazine*, vol. 11, no. 4, 2023.
- [8] A. Radford *et al.*, “Learning transferable visual models from natural language supervision,” in *International Conference on Machine Learning*, 2021.
- [9] F. Liu, D. Chen, Z.-R. Guan, X. Zhou, J. Zhu, and J. Zhou, “Remote-CLIP: A Vision Language Foundation Model for Remote Sensing,” *IEEE Transactions on Geoscience and Remote Sensing*, vol. 62, 2023.
- [10] J. D. Silva, J. Magalhães, D. Tuia, and B. Martins, “Multilingual Vision-Language Pre-training for the Remote Sensing Domain,” in *Proceedings of ACL International Conference on Advances in Geographic Information Systems*, 2024.
- [11] H. Liu, C. Li, Q. Wu, and Y. J. Lee, “Visual Instruction Tuning,” in *Proceedings of International Conference on Neural Information Processing System*, 2023.
- [12] J. Chen *et al.*, “MiniGPT-v2: large language model as a unified interface for vision-language multi-task learning,” 2023. [Online]. Available: <https://arxiv.org/abs/2310.09478>
- [13] W. Dai *et al.*, “InstructBLIP: Towards General-purpose Vision-Language Models with Instruction Tuning,” in *Proceedings of International Conference on Neural Information Processing System*, 2023.
- [14] Y. Hu, J. Yuan, C. Wen, X. Lu, Y. Liu, and X. Li, “RSGPT: A remote sensing vision language model and benchmark,” *ISPRS Journal of Photogrammetry and Remote Sensing*, vol. 224, 2025.
- [15] K. Kuckreja, M. S. Danish, M. Naseer, A. Das, S. Khan, and F. S. Khan, “GeoChat: Grounded large vision-language model for remote sensing,” in *Proceedings of IEEE Conference on Computer Vision and Pattern Recognition*, 2024.
- [16] Y. Zhan, Z. Xiong, and Y. Yuan, “SkyEyeGPT: Unifying remote sensing vision-language tasks via instruction tuning with large language model,” *ISPRS Journal of Photogrammetry and Remote Sensing*, vol. 221, 2025.
- [17] D. Muhtar, Z. Li, F. Gu, X. Zhang, and P. Xiao, “LHRS-bot: Empowering remote sensing with VGI-enhanced large multimodal language model,” in *Proceedings of European Conference on Computer Vision*, 2024.
- [18] J. A. Irvin *et al.*, “TeoChat: A large vision-language assistant for temporal earth observation data,” in *Proceedings of International Conference on Learning Representations*, 2024.
- [19] R. Ramos and B. Martins, “Using neural encoder-decoder models with continuous outputs for remote sensing image captioning,” *IEEE Access*, vol. 10, 2022.
- [20] Q. Cheng, H. Huang, Y. Xu, Y. Zhou, H. Li, and Z. Wang, “NWPU-captions dataset and MLCA-net for remote sensing image captioning,” *IEEE Transactions on Geoscience and Remote Sensing*, vol. 60, 2022.
- [21] Z. Yang, Q. Li, Y. Yuan, and Q. Wang, “HCNet: Hierarchical feature aggregation and cross-modal feature alignment for remote sensing image captioning,” *IEEE Transactions on Geoscience and Remote Sensing*, vol. 62, 2024.
- [22] H. Huang *et al.*, “MC-Net: multi-scale contextual information aggregation network for image captioning on remote sensing images,” *International Journal of Digital Earth*, vol. 16, 2023.
- [23] C. Yang, Z. Li, and L. Zhang, “Bootstrapping interactive image–text alignment for remote sensing image captioning,” *IEEE Transactions on Geoscience and Remote Sensing*, vol. 62, 2024.
- [24] Y. Cao, J. Yan, Y. Tang, Z. He, K. Xu, and Y. Cheng, “Aware-Transformer: A Novel Pure Transformer-Based Model for Remote Sensing Image Captioning,” in *Proceedings of Computer Graphics International Conference*, 2023.
- [25] R. Du *et al.*, “From plane to hierarchy: Deformable Transformer for remote sensing image captioning,” *IEEE Journal of Selected Topics in Applied Earth Observations and Remote Sensing*, vol. 16, 2023.
- [26] A. Zeng *et al.*, “Socratic Models: Composing Zero-Shot Multimodal Reasoning with Language,” in *Proceedings of International Conference on Learning Representations*, 2022.
- [27] R. P. Ramos, D. Elliott, and B. Martins, “Retrieval-augmented Image Captioning,” in *Proceedings of Conference of the European Chapter of the ACL*, 2023.
- [28] R. Ramos, B. Martins, D. Elliott, and Y. Kementchedjhiya, “SmallCap: Lightweight Image Captioning Prompted with Retrieval Augmentation,” in *Proceedings of IEEE Conference on Computer Vision and Pattern Recognition*, 2023.
- [29] A. A. Hagberg, D. A. Schult, and P. J. Swart, “Exploring network structure, dynamics, and function using NetworkX,” in *Proceedings of the Python in Science Conference*, 2008.
- [30] J. Hessel, A. Holtzman, M. Forbes, R. L. Bras, and Y. Choi, “CLIP-Score: A Reference-free Evaluation Metric for Image Captioning,” in *Proceedings of Conference on Empirical Methods in Natural Language Processing*, 2022.

- [31] M. Caron *et al.*, “Emerging Properties in Self-Supervised Vision Transformers,” in *Proceedings of IEEE International Conference on Computer Vision*, 2021.
- [32] D. M. Alves *et al.*, “Tower: An Open Multilingual Large Language Model for Translation-Related Tasks,” 2024. [Online]. Available: <https://arxiv.org/abs/2402.17733>
- [33] P. H. Martins *et al.*, “EuroLLM: Multilingual Language Models for Europe,” 2024. [Online]. Available: <https://arxiv.org/abs/2409.16235>
- [34] G. Team *et al.*, “Gemma 3 Technical Report,” Google, Tech. Rep., 2025.
- [35] T. Wolf *et al.*, “HuggingFace’s Transformers: State-of-the-art Natural Language Processing,” 2020. [Online]. Available: <https://arxiv.org/abs/1910.03771>
- [36] X. Lu, B. Wang, X. Zheng, and X. Li, “Exploring Models and Data for Remote Sensing Image Caption Generation,” *IEEE Transactions on Geoscience and Remote Sensing*, vol. 56, 2017.
- [37] B. Qu, X. Li, D. Tao, and X. Lu, “Deep semantic understanding of high resolution remote sensing image,” in *Proceedings of International Conference on Computer, Information and Telecommunication Systems*, 2016.
- [38] DeepSeek-AI *et al.*, “DeepSeek-R1: Incentivizing Reasoning Capability in LLMs via Reinforcement Learning,” DeepSeek, Tech. Rep., 2025.